ISSN: 1813-162X (Print) ; 2312-7589 (Online)

Tikrit Journal of Engineering Sciences

available online at: http://www.tj-es.com

College of Engineering

TJES Tikrit Journal of Engineering Sciences

# Control Techniques of Torque Ripple Minimization for Induction Motor

**Thamir Hassan Atyia ***

Department of Electrical Engineering
College of Engineering
Tikrit University
Salahuddin
Iraq

***Keywords*:**

Induction motor
torque ripple
direct torque control

**ARTICLE INFO**

***Article history:***

| | |
|---|---|
| Received | 22 May 2018 |
| Accepted | 28 November 2018 |
| Available online | 01 December 2018 |



**A B S T R A C T**

A Matlab-Simulink environment used to build a model of an Induction Motor (IM) to study and explore methods for minimizing the torque ripple. Various control strategies were reviewed and simulation studies were carried out for the following control methods: Direct Torque control, Direct Torque control with harmonic elimination, and Direct Torque control with Matrix convertor were the obtained results analyzed, evaluated, and compared to each other. The simulation results confirmed that Using Direct Torque Control with Harmonic elimination method was significantly minimized the torque ripple as the harmonics of the output voltage were canceled; discussions and conclusions were presented in this study.



DOI: http://dx.doi.org/10.25130/tjes.25.4.10

## تقنيات لتقليل تموج عزم الدوران للمحرك الحثي

**الخلاصة**

إن وجود بيئة ماتلاب-SIMULINK تستخدم لبناء نموذج لمحرك حثي (IM) لدراسة واستكشاف طرق لتقليل تموج عزم الدوران. وتم استعراض استراتيجيات مختلفة وأجريت دراسات محاكاة لطرق التحكم التالية: التحكم المباشر في عزم الدوران: التحكم المباشر في عزم الدوران مع حاذف الاشارة التوافقية، والتحكم المباشر في عزم الدوران مع حاذف الاشارة التوافقية مع مصفوفة محول((AC-AC وكانت النتائج المتحصل عليها تم تحليلها وتقييمها، ومقارنتها مع بعضها البعض. أكدت نتائج المحاكاة التي تم تحقيقها عن تقليل التموج في عزم الدوران؛ وتم عرض المناقشات والاستنتاجات والاقتراحات في هذه الدراسة.

## 1. INTRODUCTION

Induction motors can benefit from their mechanical construction the following advantages simple and rugged structure, low-cost, low overhead maintenance also manufactured for wide range of constant speed industrial applications.

Takahashi and Ngouchi [1] present a method called direct torque control (DTC) by controlling flux and torque values using optimization-switching routine. Lascu et al. [2] introduced a new direct torque and flux control based on space vector modulation (DTC-SVM). Huangang et al. [3] have presented a control technique achieved good performance using variable structure control of electrical torque and stator flux. Venkata and Panda [4] claimed drive efficiency increase by reducing switching frequency compared to the normal DTC. Rajendran and Devarajan [5] to reduce the ripple in steady state DTC-SVM is proposed, the simulation and experimental results confirmed that the novel proposed scheme able to produce good dynamic response. Kumar et al. [6] studied practicality of using induction motor drive under different abnormal Voltage conditions with matrix converter. Rakan and Allu [7] illustrate the effectiveness of using Artificial Neural Network (ANN) technique to improve speed and torque control of a separately excited DC machine drive without speed or torque sensors. Abdelelah and Fatah [8] show enhanced improvement of the Fuzzy Logic Controller with fast response and the effect of load as a disturbance on the shaft of the motor has been rejected quickly. Youns and Hassan [9] presents the performance analysis and simulation of a Sinusoidal pulse width Modulation (SPWM) inverter-fed three-phase induction motor under some fault conditions. This research studies applied three different techniques for minimizing torque ripple of

* Corresponding E-mail: dr.thamir.atyia@tu.edu.iq

Induction Motor namely: Direct Torque Control, Direct Torque Control with Harmonic elimination, and Direct Torque Control with Harmonic elimination and Matrix convertor.

## 2. INDUCTION MOTOR CONTROL

For simplicity, the induction motor considered will have the following assumptions [10]:

- Three phase windings of symmetrical two-pole.
- Ignored slotting effects.
- Infinite permeability of the iron parts.
- Radial flux density in the air gap.
- Neglected iron losses.
- Stator and rotor windings treated as a single, multi-turn full pitch coil situated on the two sides of the air gap."

### 2.1. Voltage equations

In this, section stator voltages presented to stationary fixed reference frame to the stator as explained in Eqs. (1)-(3) [10].

$$V_{sA} = R_s i_{sA}(t) + \frac{d\psi_{sA}(t)}{dt} \quad (1)$$

$$V_{sB} = R_s i_{sB}(t) + \frac{d\psi_{sB}(t)}{dt} \quad (2)$$

$$V_{sC} = R_s i_{sC}(t) + \frac{d\psi_{sC}(t)}{dt} \quad (3)$$

Similarly, the rotor voltages according to the rotating frame fixed to the rotor as in Eqs. (4)-(6) [10].

$$V_{rA} = R_r i_{rA}(t) + \frac{d\psi_{rA}(t)}{dt} \quad (4)$$

$$V_{rB} = R_r i_{rB}(t) + \frac{d\psi_{rB}(t)}{dt} \quad (5)$$

$$V_{rC} = R_r i_{rC}(t) + \frac{d\psi_{rC}(t)}{dt} \quad (6)$$

### 2.2. Park's Transform

The Park's transform applied to reduce equation voltages given in Eqs. (1)-(6) and obtain constant coefficients in the differential equations. Physically, it

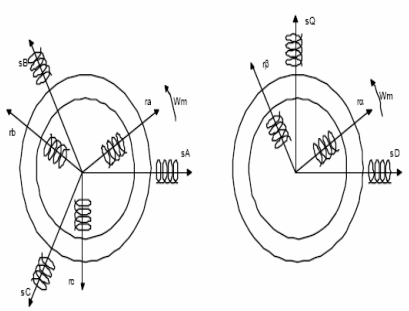


**Fig. 1.** Park's transform e of equivalent axis transformation.

transforming the three windings of the induction motor to just two windings, as depicted in Fig. 1 [3].

For symmetrical three-phase machine, equivalence for direct (D) and quadrature (Q) magnitudes with the magnitudes per phase are as follows [10]:

$$\begin{bmatrix} V_{sD} \\ V_{sQ} \\ V_{s0} \end{bmatrix} = c. \begin{bmatrix} \cos\theta & \cos(\theta - 2\pi/3) & \cos(\theta + 2\pi/3) \\ -\sin\theta & -\sin(\theta - 2\pi/3 & -\sin(\theta + 2\pi/3) \\ 1/\sqrt{2} & 1/\sqrt{2} & 1/\sqrt{2} \end{bmatrix} \begin{bmatrix} V_{sA} \\ V_{sB} \\ V_{sC} \end{bmatrix} \quad (7)$$

$$\begin{bmatrix} V_{sA} \\ V_{sB} \\ V_{sC} \end{bmatrix} = c. \begin{bmatrix} \cos\theta & -\sin\theta & 1/\sqrt{2} \\ \cos(\theta - 2\pi/3) & -\sin(\theta - 2\pi/3 & 1/\sqrt{2} \\ \cos(\theta + 2\pi/3) & -\sin(\theta + 2\pi/3) & 1/\sqrt{2} \end{bmatrix} \begin{bmatrix} V_{sD} \\ V_{sQ} \\ V_{s0} \end{bmatrix} \quad (8)$$

where "c" is a constant of values 2/3 or 1 for the so-called non-power invariant form or the value $\sqrt{2/3}$ for the power-invariant quantities.

### 2.3. Torque Expressions

The general expression for the torque is as follows [10]:

$$T_e = c\,\psi_s . i_r \quad (9)$$

where c is a constant, $i_r$ and $\psi_s$ are the space phasor of the rotor current and stator flux respectively referred to the stationary reference frame fixed to the stator. Eq. (9) also expressed as follows:

$$T_e = c|\psi_s||i_r|\sin\gamma \quad (10)$$

where γ is the existing angle between the stator flux linkage and the rotor current.

### 2.4. Direct Torque Control Technique

For a three phase induction motor the instantaneous electromagnetic torque is proportional to the cross product of the current space vector and the stator flux linkage space vector as:

$$T_e = \frac{3}{2} p\,\bar{\psi}_s \times \bar{i}_s \quad (11)$$

$$\bar{\psi}_s = |\bar{\psi}_s| e^{j\rho_s} \quad (12)$$

$$\bar{i}_s = |\bar{i}_s| e^{j\alpha_s} \quad (13)$$

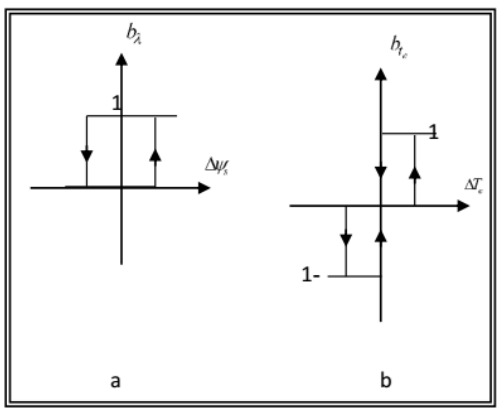


**Fig. 2**. Characteristics of (a) flux controller, and (b) torque controller.

where

$\bar{\psi}_s$ is the stator flux-linkage space vector.

$\bar{i}_s$ is the stator-current space vector.

$\rho_s$ is the stator flux-linkage space vector angle with respect to the direct torque axis of stator reference frame.

$\alpha_s$ is the stator current space vector angle with respect to the direct axis of stator reference frame.

$$T_e = \frac{3}{2} p \cdot |\bar{\psi}_s| \cdot |\bar{i}_s| \sin(\alpha_s - \rho_s) \quad (14)$$

$$T_e = \frac{3}{2} \cdot p \cdot |\bar{\psi}_s| \cdot |\bar{i}_s| \cdot \sin(\alpha) \quad (15)$$

In direct torque control the switching vector are selected on the basis of keeping the stator flux-linkage error within tolerance limit and keeping the torque error within tolerance limit and their width are $2\Delta\psi_s$ and $2\Delta t_e$, respectively.

Two independent hysteresis controllers control the amplitudes of stator flux and motor torque. The feedback signals, $T_e$ and $|\psi_s|$, are computed from stator voltages and currents. The motor emf space vector was integrated to obtain stator flux linkage space vector $\bar{\psi}_s$ [10].

$$\bar{\psi}_s = \int (\bar{v}_s - R_s \bar{i}_s) \cdot dt \quad (16)$$

DC link voltage $V_{dc}$ been used to calculate the stator voltage space vector $\bar{v}_s$ and the stator current space vector $\bar{i}_s$ is calculated from measured currents $i_a$, $i_b$, and $i_c$.

$$\bar{i}_s = \frac{2}{3} \cdot \left[ i_a + i_b \cdot e^{j\frac{2\pi}{3}} + i_c \cdot e^{j\frac{4\pi}{3}} \right] \quad (17)$$

The flux linkage and torque errors, $\Delta\psi_s$ and $\Delta t_e$, are applied to respective two controllers, whose characteristics are shown in Fig. 2. The output signal of the controller; $b_\lambda$ with flux values of 0 and 1, and that $b_{te}$, of the torque controller output with values of -1, 0, and 1. The selection of the inverter states (switching vector) depends on the values of $b_\lambda$ and $b_{te}$, it also depends on the flux angle, i.e. sector position.

#### 2.4.1. Stator Flux Linkage Estimator

To achieve stability and proper operation in vector controlled induction motor drive an accurate flux estimation is required by using various estimation techniques: applying voltage model, current model, or combination of both. Only stator resistance used with voltage model, the first principles of DTC [11] as:

$$\psi_{s\alpha} = \int (v_{s\alpha} - i_{s\alpha} R_s) \cdot dt \quad (18)$$

$$\psi_{s\beta} = \int (v_{s\beta} - i_{s\beta} R_s) \cdot dt \quad (19)$$

The voltage model at high speed achieves accurate estimation on the other hand at low speed the method has some drawbacks. The Eqs. (18)-(19) depicts that the stator flux linkage is a time integral of stator electromotive force as:

$$e_s = V_s - R_s i_s \quad (20)$$

Employed electronic circuits' d.c. drift caused by noise and selecting improper initial values of stator flux linkage leads to saturation of integrator this complicated the process of estimation of $\psi_s$ based on integration of $e_s$ under sinusoidal steady-state condition Eqs. (18)-(19) are reduced to

$$jw_e \cdot \bar{\psi}_{s\alpha} = \bar{V}_s - \bar{I}_{s\alpha} \cdot R_s \quad (21)$$

$$jw_e \cdot \bar{\psi}_{s\beta} = \bar{V}_s - \bar{I}_{s\beta} \cdot R_s \quad (22)$$

or in vector notation

$$jw_e \cdot \bar{\psi}_s = \bar{V}_s - \bar{I}_s \cdot R_s \quad (23)$$

$$\bar{\psi}_s = \frac{\bar{V}_s - \bar{I}_s \cdot R_s}{jw_e} \quad (24)$$

where $w_e$ is the synchronous frequency.

### 2.5. Harmonic Elimination PWM Technique

To minimize the harmonic components within the inverter output voltage an approach has been developed in the early 1960's based on a pre calculated PWM. Bowes [12] presented harmonic elimination PWM technique that led to significant reduction of the induction motor torque ripple and large reduction of the harmonic in the AC main output voltage without increasing the number of switches per period.

### 2.6. Principles of the Matrix convertor

In [13] Akihiro Odaka proposed a method called matrix convertor that sets semiconductor switches into a matrix configuration then controls them for the conversion of input AC voltages to the desired AC voltage directly and with AC, bi-directional switches are required.

## 3. SIMULATION RESULTS AND DISCUSSION

To verify the effectiveness of the proposed simulation model based on *POWERSYS* and *SIMULINK*, some simulation results for different control methods are provided and compared with each other. The following motor parameters were used to build the simulation model as: 6/4 3 phase, power rate = 150 kw, resistance of stator = 0.01485 ohm, leakage inductance of stator = 0.0003027 henry, resistance of rotor = 0.009295 ohm, leakage inductance of rotor = 0.0003027 henry, mutual inductance = 0.01064, inertia = 3.1 kg.m$^2$, friction = 0.08 N.m.s, voltage = 460, frequency = 60.

Various control strategies were studied, the Matlab-Simulink models, and the simulation results were analyzed and discussed as follows [14,15].

### 3.1. Direct Torque Control

In this section model of the Direct Torque Control method for the specified motor was built in Simulink block diagram as shown in Fig. 3.

Samples of the simulation results are presented in Fig. 4 shown the stator flux, stator current, rotor speed and electromagnetic torque. Fig. 5 zoomed in section of the simulation results for detailed investigations which shows that the band of the torque ripple is approximately from 950 to 1050 N m as the reference torque is 1000 N m.

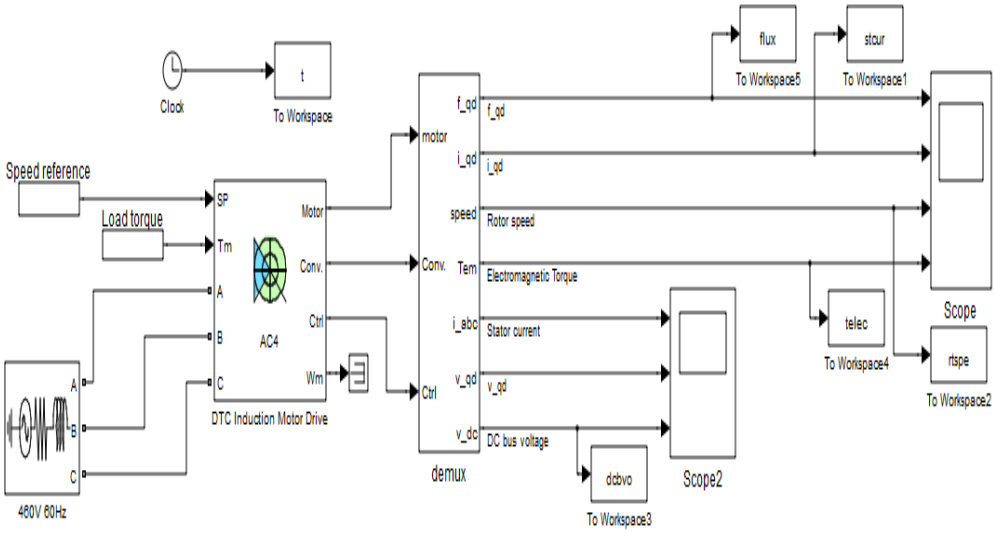


**Fig. 3.** Block diagram for IM with DTC.

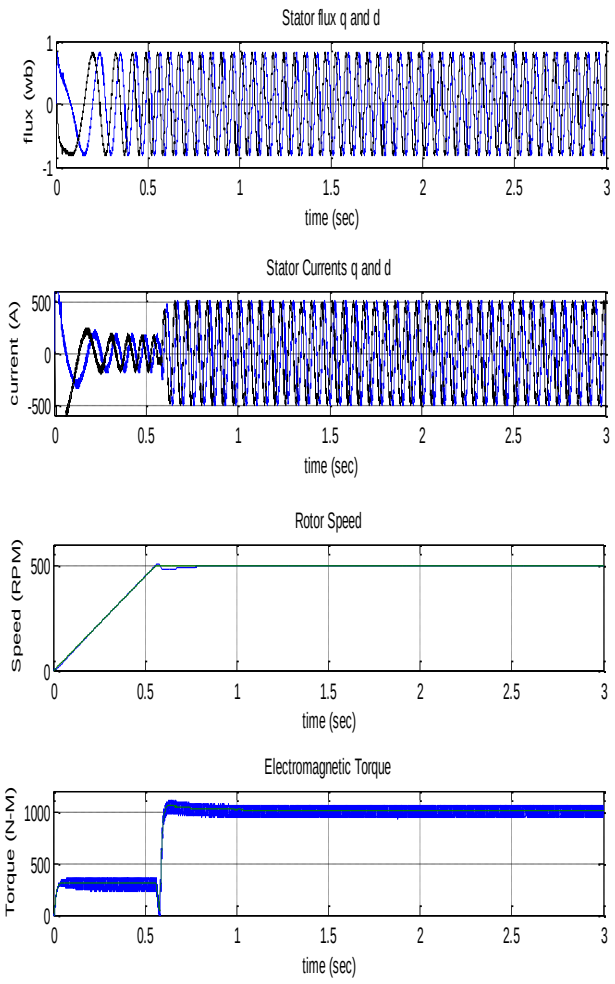


**Fig. 4.** IM performance with DTC.

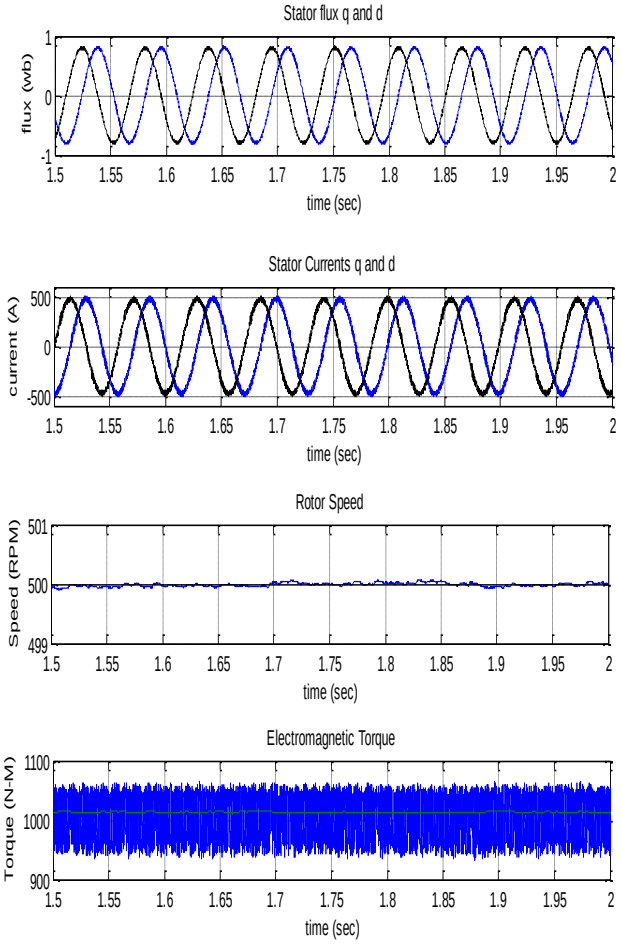


**Fig. 5.** IM performance with DTC (zoomed in).

### *3.2. Direct Torque Control with Harmonic Elimination*

In this section model of the Direct Torque Control with Harmonic elimination method for the specified motor was built in Simulink block diagram as shown in Fig. 6.

Samples of the simulation results are presented in Fig. 7 shown the stator flux, stator current, rotor speed and electromagnetic torque. Fig. 8 zoomed in section of the simulation results for detailed investigations, which shows that the band of the torque ripple is approximately from 960 to 1010 N m as the reference torque is 1000 N m.

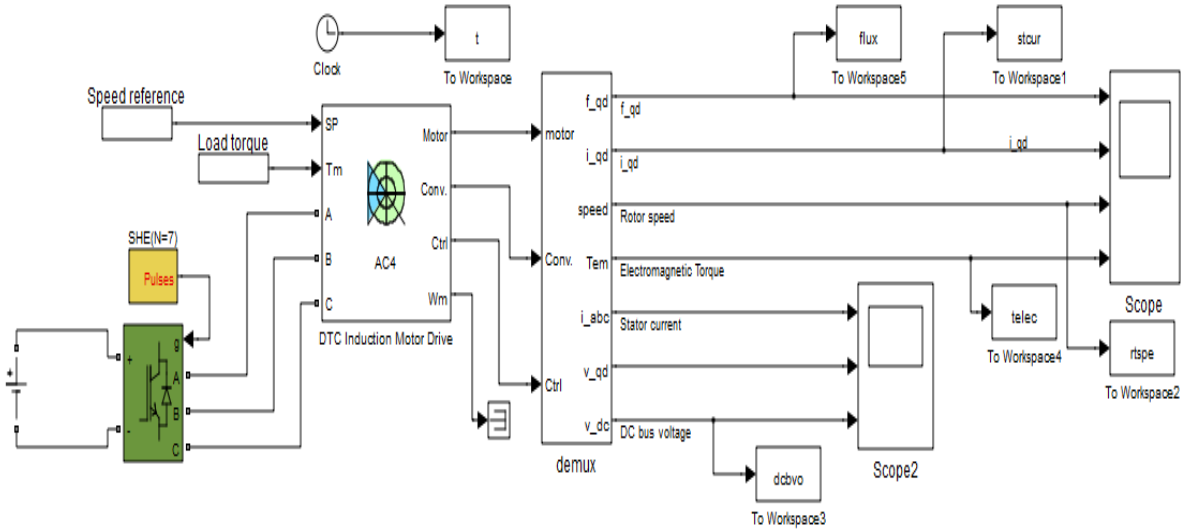


**Fig. 6.** Block diagram for IM with DTC and harmonic elimination.

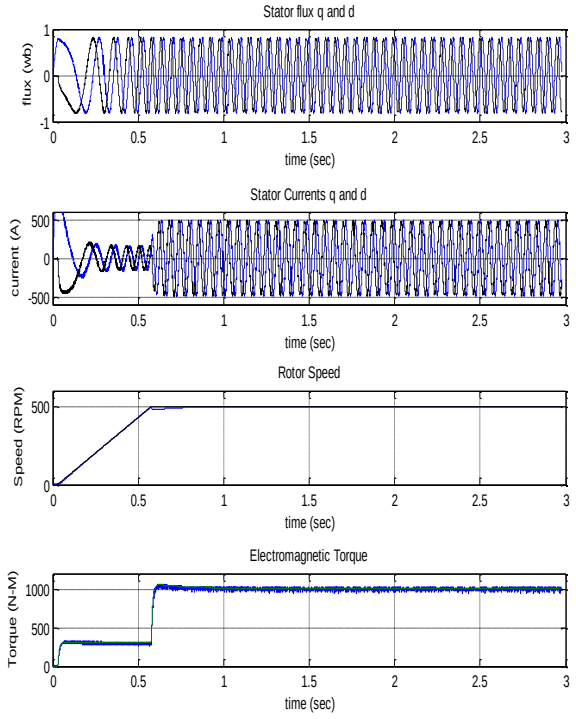


**Fig. 7.** IM performance with DTC and Harmonic elimination.

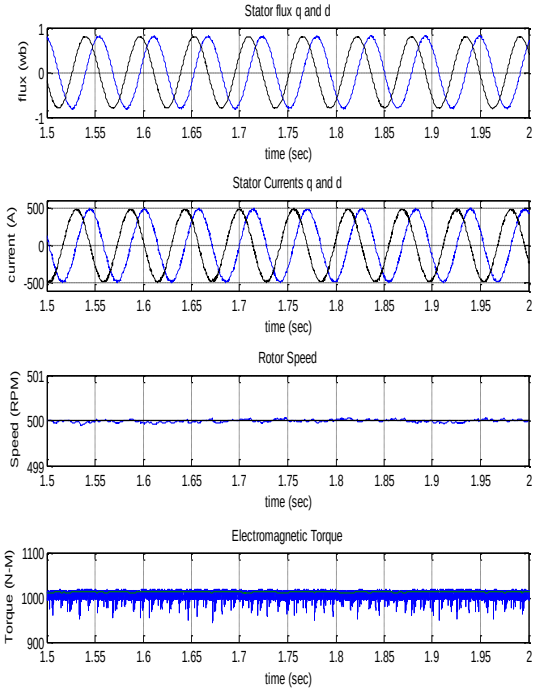


**Fig. 8.** IM performance with DTC and Harmonic elimination (zoomed in).

### *3.3. Direct Torque Control with Harmonic Elimination and Matrix Convertor*

In this section model of the Direct Torque Control with Harmonic elimination and Matrix Convertor method for the specified motor was built in Simulink block diagram as shown in Fig. 9.

Samples of the simulation results are presented in figure 10 shown the stator flux, stator current, rotor speed and electromagnetic torque. Fig. 11 zoomed in section of the simulation results for detailed investigations which shows that the band of the torque ripple is approximately from 960 to 1005 Nm as the reference torque is 1000 Nm. It can be notice that the frequency of high torque variations was dramatically reduced.

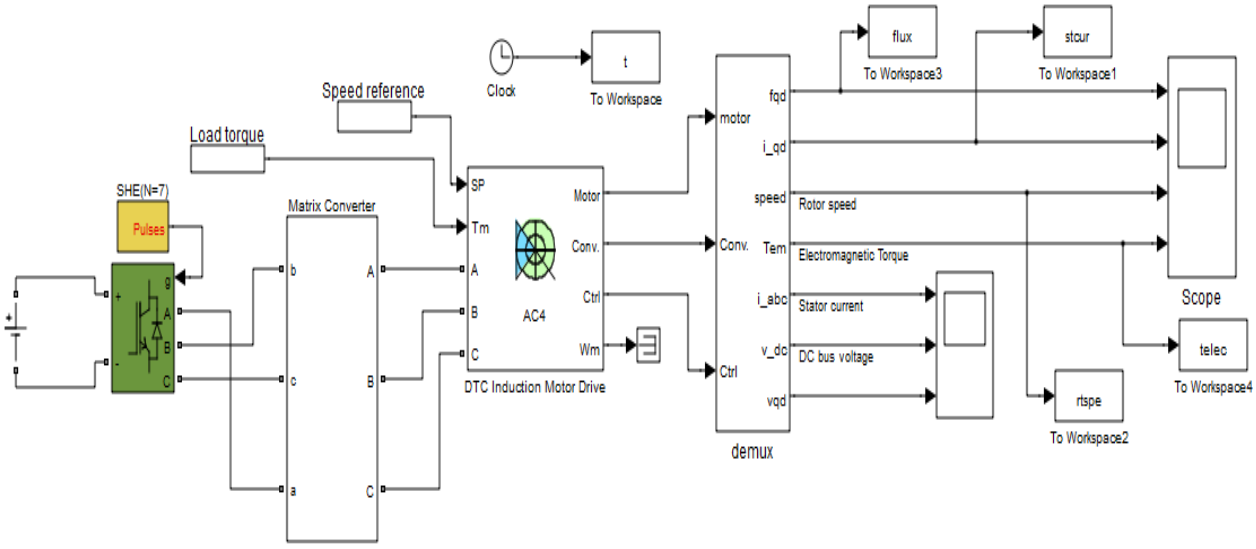


**Fig. 9.** Block diagram for IM with DTC, Harmonic elimination and matrix convertor.

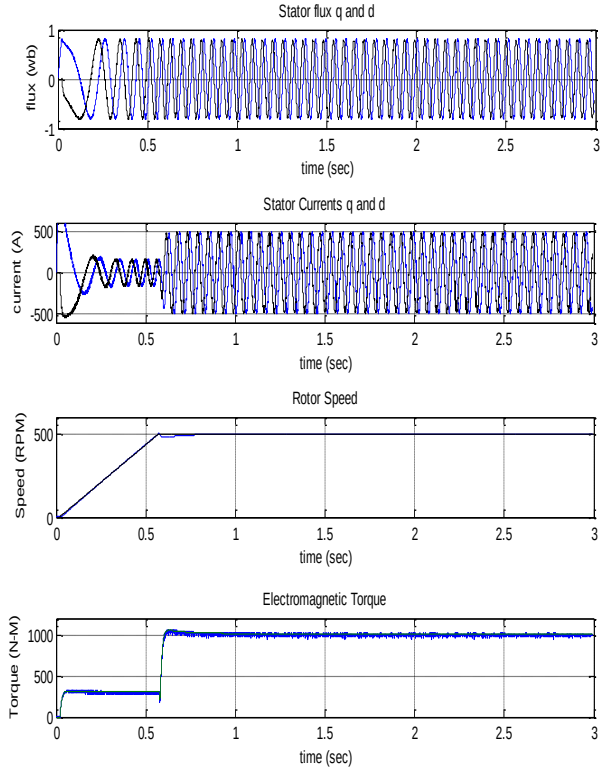


**Fig. 10.** IM performance with DTC with Harmonic elimination and Matrix Convertor.

## 4. CONCLUSIONS

In this research study a Matlab-Simulink, based modeling was presented to visualize the teaching of modeling subjects and enhance research exploration. The modeling process provide means of results analysis and the proper tackle action. This simulation program offers a better understanding of the induction motor dynamic behaviour and benefiting from the following advantages: safety process, saving in time, and saving in cost. In this study, the results obtained from the dynamic analysis of an induction motor may be summarized as follows:

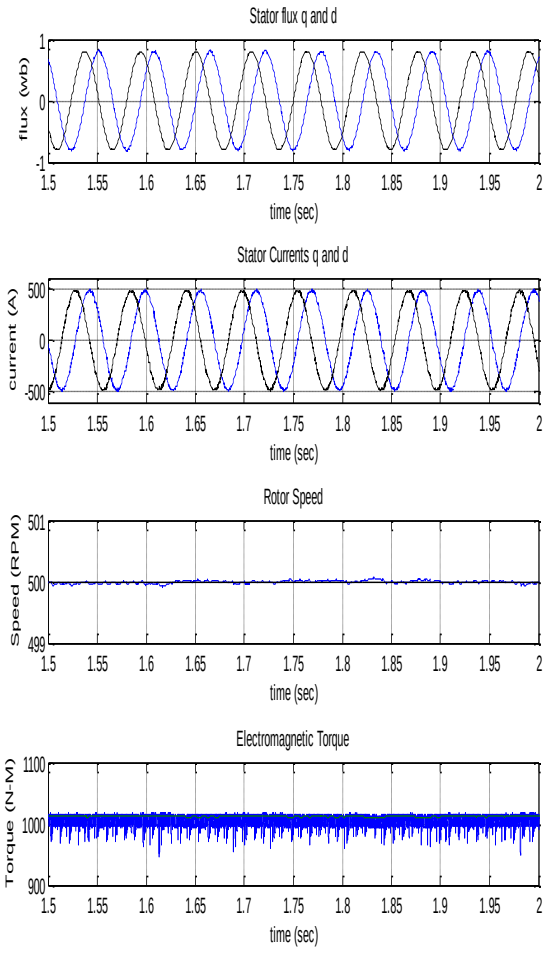


Fig. 11. IM performance with DTC with Harmonic elimination and Matrix Convertor (zoomed in).

- The torque ripple when using Direct Torque Control method is larger compared to other used methods.
- Using Direct Torque Control with Harmonic elimination method was significantly minimized the

torque ripple as the harmonics of the output voltage were canceled.

- Little further improvements were achieved by using Direct Torque Control with Harmonic elimination and Matrix convertor method in compare with the Direct Torque Control with Harmonic elimination.

## REFERENCES


[1] Takahashi I, Noguchi T. A new quick response and high efficiency control strategy of an induction motor. *IEEE Transactions on Industry Applications* 1989; **IA22** (5): 820-827.

[2] Lascu C, Boldea I, Blaabjerg F. A modified direct torque control for induction motor sensorless drive. *IEEE Transactions on Industry Applications* 2000; **IA36** (1): 122-130.

[3] Huangang W, Wenli X, Geng Y, Jian L. Variable structure torque control of induction motor using space vector modulation. *Electrical Engineering* 2005; **87**(2): 93-102.

[4] Venkata G, Panda A. Torque ripple reduction in direct controlled induction motor drive using fuzzy logic. *National Institute of Technology Rourkela* 2007.

[5] Rajendran R, Devarajan N. Simulation and implementation of a high performance torque control scheme of induction motor. *International Journal of Electrical and Computer Engineering* 2012; **2**(3): 277-284.

[6] Kumar V, Bansal RC, Joshi RR. Experimental realization of matrix converter based induction motor. *International Journal of Control, Automation, and Systems* 2008; **6**(5): 670-676.

[7] Antar RK, Allu AA. Sensorless speed/torque control of DC machine using artificial neural network technique. *Tikrit Journal of Engineering Sciences* 2016; **23**(3): 55-62.

[8] Abdelelah KM, Fatah AA. Real time speed control of DC motor by programming the fuzzy controller in C language. *Tikrit Journal of Engineering Sciences* 2016; **23**(3): 91-95.

[9] Youns YM, Hassan OM. Performances analysis of SPWM inverter-fed three phase induction motor during fault conditions. *Tikrit Journal of Engineering Sciences* 2016; **23**(3): 55-62.

[10] Boldea I, Nasar S. The induction machine handbook. 2002, CRC press.

[11] Ozkop E. Direct torque control of induction motor using space vector modulation.*12th International Power System Conference* 2008; 12-15 May: pp. 368-372.

[12] Bowes SR. Novel space vector based harmonic elimination inverter control. *IEEE Transactions on Industry applications* 2000; **36**(2): 549-557.

[13] Odaka A. High efficiency power conversion using a matrix convertor. *Fuji Electric Review* 2004; **50**(3): 94-98.

[14] Matlab user manual, Math works Inc., 2014.

[15] Simulink user manual, Math works Inc., 2014.